J|A|C|S
ARTICLES
Published on Web 04/01/2006

Two-Site Ionic Labeling with Pyranine: Implications for Structural Dynamics Studies of Polymers and Polypeptides by Time-Resolved Fluorescence Anisotropy

Jai Sharma, Dina Tleugabulova, Wojciech Czardybon, and John D. Brennan*

Contribution from the Department of Chemistry, McMaster University, Hamilton, ON, L8S 4M1, Canada

Received December 22, 2005; E-mail: brennanj@mcmaster.ca

Abstract: Time-resolved fluorescence anisotropy (TRFA) is widely used to study dynamic motions of biomolecules in a variety of environments. However, depolarization due to rapid side chain motions often complicates the interpretation of anisotropy decay data and interferes with the accurate observation of segmental motions. Here, we demonstrate a new method for two-point ionic labeling of polymers and biomolecules that have appropriately spaced amino groups using the fluorescent probe 8-hydroxyl-1,3,6-trisulfonated pyrene (pyranine). TRFA analysis shows that such labeling provides a more rigid attachment of the fluorophore to the macromolecule than the covalent or single-point ionic labeling of amino groups, leading to time-resolved anisotropy decays that better reflect the backbone motion of the labeled polymer segment. Optimal coupling of pyranine to biomolecule dynamics is shown to be obtained for appropriately spaced Arg groups, and in such cases the ionic binding is stable up to 150 mM ionic strength. TRFA was used to monitor the behavior of pyranine-labeled poly(allylamine) (PAM) and poly-D-lysine (PL) in sodium silicate derived sol−gel materials and revealed significant restriction of backbone motion upon entrapment for both polymers, an observation that was not readily apparent in a previous study with entrapped fluorescein-labeled PAM and PL. The implications of these findings for fluorescence studies of polymer and biomolecule dynamics are discussed.

Introduction

The use of fluorescence methods to monitor the dynamics of biomolecules often requires that the biomolecule of interest be labeled with an extrinsic fluorescent dye. While the vast majority of fluorescence labeling is achieved by covalent attachment of fluorophores to a biomolecule, this method of labeling may compromise protein activity and function due to the harsh conditions required to carry out the labeling reaction.[1] As an alternative, noncovalent labeling through ionic, hydrophobic, hydrogen bonding, or donor−acceptor interactions is attracting interest, as these methods better preserve protein function and activity, require less time, can be done at physiological pH, and do not require purification steps when the stoichiometry of the complex is known.[1,2] The viability of such noncovalent labeling, however, is dependent on the biomolecule having surface accessible residues or side chains that can bind dyes with high efficiency and selectivity.

Lysine, glutamic acid, and arginine have the highest frequency of occurrence among the common amino acids found on protein surfaces,[3] and hence these amino acids provide the best opportunity for noncovalent labeling of proteins. Specifically, lysine and arginine have cationic side chains that are appropriate for selective labeling using anionic fluorophores. These residues form strong ionic complexes with sulfonate dyes,[4,5] which are ideal for fluorescence measurements[6] since these ionic complexes exhibit high emission intensity due to ionization of the probe.[7] However, the side chain length of these residues creates a significant drawback when studying backbone motions of a protein using either covalent or ionic fluorescent labels. A long linker can cause the probe to experience motions that are independent of the protein backbone due to high flexibility at the site of attachment[8] and can decouple the probe motion from the peptide backbone motion.[9] Indeed, reduction in linker length has led to improved measurements of the segmental motions near the residue to which the probe is attached in both covalently[10] and ionically labeled systems;[9] however, these findings may not be generally applicable to the study of protein segmental or backbone motions where attachment of the probe via a short linker is not an option.

An alternative approach to reduce independent probe motions is to use bifunctional labels that tether the probe to the

(1) Patonay, G.; Salon, J.; Sowell, J.; Strekowski, L. *Molecules* **2004**, *9*, 40−49.
(2) Colyer, C. *Cell Biochem. Biophys.* **2000**, *33*, 323−337.
(3) Xu, G.; Takamoto, K.; Chance, M. R. *Anal. Chem.* **2003**, *75*, 6995−7007.
(4) Salih, B.; Zenobi, R. *Anal. Chem.* **1998**, *70*, 1536−1543.
(5) Matulis, D.; Lovrien, R. *Biophys. J.* **1998**, *74*, 422−429.
(6) Haugland, R. P. In *Handbook of Fluorescent Probes and Research Chemicals*, 6th ed; Spence, M. Z., Ed.; Molecular Probes Inc: Eugene, OR, 1996.
(7) Gutman, M.; Nachliel, E.; Huppert, D. *Eur. J. Biochem.* **1982**, *125*, 175−181.
(8) Tao, T. *FEBS Lett.* **1978**, *93*, 146−150.
(9) Tleugabulova, D.; Czardybon, W.; Brennan, J. D. *J. Phys. Chem. B* **2004**, *108*, 10692−10699.
(10) Cohen, B. E.; Pralle, A.; Yao, X.; Swaminath, G.; Gandhi, C. S.; Jan, Y. N.; Kobilka, B. K.; Isacoff, E. Y.; Jan, L. Y. *Proc. Natl. Acad. Sci.* **2005**, *102*, 965−970.

10.1021/ja058707e CCC: $33.50

biomolecule at two sites, thereby reducing probe flexibility.[11,12] The success of this approach has previously been demonstrated in EPR studies[13] and fluorescence studies[14,15] and has the advantage of allowing the measurement of slow (microsecond) rotational motions of biomolecules using covalent bifunctional probes, as outlined in detail by Corrie et al.[11] While there are some reports of the use of bifunctional probes to measure protein dynamics,[12,16] this technique has not been widely employed for protein dynamics studies using time-resolved fluorescence anisotropy (TRFA), likely because many of these dyes are Cys-reactive and require the presence of two closely spaced, surface accessible cysteine residues.

Recently, extensive research using MALDI mass spectrometry[4,7,17,18] and isothermal titration calorimetry[5] has led to a better understanding of the noncovalent interaction between basic amino acids and sulfonic acid ligands and has provided evidence to suggest that a two-point interaction can be achieved using a noncovalent fluorescent labeling approach. Specifically, mass spectrometry studies of protein complexes with a trisulfonated pyrene probe have shown that fewer dye/protein adducts were formed than expected given the number of surface accessible arginine residues, a result that suggested a complex of two arginine residues per single sulfonated pyrene molecule.[18] Other evidence has shown electrostatic binding of 8-hydroxyl-1,3,6-trisulfonated pyrene (pyranine) to proteins through all three sulfonate groups.[7,19,20]

While the multisite electrostatic interaction between trisulfonic acid derivatized fluorophores and basic residues has proven to be of limited use for mapping protein surfaces by mass spectrometry,[18] we demonstrate that it can be advantageous in TRFA measurements, as it significantly reduces rapid probe motions arising from the flexible linker between the probe and protein[9,10] (i.e., an amino acid side chain) or flexibility of the probe at its point of attachment.[8] In the present work, we use TRFA to probe segmental motions of homogeneous polyamines using single-point and double-point ionic labeling with fluorescein and pyranine, respectively, and show that the reduction of independent probe motions resulting from a double-point ionic interaction leads to a closer correspondence between segmental motions measured using TRFA and NMR spectroscopy, particularly in cases where appropriately spaced Arg residues are present.

To demonstrate the utility of this labeling method the segmental mobility of polyamines entrapped in sodium silicate derived hydrogels was assessed using both fluorescein- and pyranine-labeled polymers. Vast interest in the field of protein encapsulation using the sol−gel process merits such studies, as a clear understanding of the effects of sol−gel entrapment on protein dynamics can provide important information on how such encapsulation influences protein function and activity. The charged polymers, poly(allylamine) and poly-D-lysine, represent suitable model systems for both flexible and rigid biomolecules entrapped in sol−gel derived materials and were selected since each is expected to undergo significant electrostatic interactions with silica, which should restrict motion. Our results suggest that pyranine-labeled polymers more accurately reflect the dynamics of cationic polymers, demonstrating the potential for using noncovalent labeling of polypeptides with pyranine to study polypeptide backbone dynamics in a wide range of environments. These studies highlight the effects that independent probe motions have on the accurate interpretation of fluorescence anisotropy decay data.

Experimental Section

Chemicals: Fluorescein was supplied by Sigma (St. Louis, MO). 8-Hydroxyl-1,3,6-trisulfonated pyrene (pyranine) was purchased from Molecular Probes (Eugene, Oregon). Sodium silicate solution (~14% NaOH, ~27% SiO_2), Dowex 50WX8-100 ion-exchange resin, poly(allylamine) (20% aqueous solution, MW 17 000, pK_a of 10.5[21]), linear poly(ethyleneimine) (M_n 13 000), poly-D-lysine hydrobromide (MW 17 000), poly-L-ornithine hydrochloride (MW 23 500), and poly-L-arginine hydrochloride (MW 26 000) were purchased from Sigma-Aldrich (Milwaukee, WI). All water was distilled and deionized using a Milli-Q Synthesis A10 water purification system. All reagents were used without further purification.

Sample Preparation: Stock solutions containing ~500 μM fluorescein in dimethylformamide or ~250 μM pyranine in water[6] were used to prepare samples containing 1.4 μM fluorescein or 2 μM pyranine and 0.05 wt % of a given polyamine in 5 mM Tris-HCl, pH 8.3. An aliquot of the stock probe solution was added to a concentrated aliquot of aqueous polyamine solution to initially form the probe−polyamine complex. The resulting solution was then diluted with water followed by buffer to reach the final concentrations noted above. Samples were analyzed in polymethacrylate fluorimeter cuvettes (transmittance curve C) obtained from Sigma.

A sodium silicate stock solution was prepared according to the procedure described by Bhatia et al.[22] Briefly, 2.9 g of sodium silicate was diluted into 10 mL of ddH_2O, and 5 g of the Dowex resin was immediately added to remove the Na^+ and adjust the pH to a value of 4.0. The mixture was stirred for 30 s and then vacuum filtered through a Buckner funnel. The filtrate was then further filtered through a 0.45 μM membrane syringe filter to remove any particulates in the solution. Sol−gel derived hydrogels (~2 wt % SiO_2) were prepared by mixing (1:4, v/v) the sodium silicate stock solution and the probe−polyamine stock solution to reach final concentrations of 5 mM Tris-HCl, ~pH 7, 0.05 wt % of the polyamine and either 1.4 μM fluorescein or 2 μM pyranine, as previously described.[9] To avoid flocculation, the pH of the preformed probe−polyamine complex was adjusted to pH ~4 with an aliquot of concentrated HCl prior to mixing with the sodium silicate stock solution. The mixtures were quickly poured into disposable polymethacrylate cuvettes to form hydrogels of dimensions 10 × 10 × 20 mm^3 and sealed with Parafilm. Samples were aged overnight prior to analysis.

Sample Analysis: Absorbance measurements were made using a Cary 400 UV−visible spectrophotometer (Varian Canada, Quebec) over the range 400−600 nm. Steady-state fluorescence anisotropy measurements were performed using an SLM 8100 spectrofluorimeter (Spectronic Instruments, Rochester, NY) as described in detail elsewhere.[9] Pyranine-labeled polymers were excited at 455 nm with emission

(11) Corrie, J. E.; Craik, J. S.; Munasinghe, R. N. *Bioconjugate Chem.* **1998**, *9*, 160−167.
(12) Mercier, P.; Ferguson, R. E.; Irving, M.; Corrie, J. E. T.; Trentham, D. R.; Sykes, B. D. *Biochemistry* **2003**, *42*, 4333−4348.
(13) Wilcox, M. D.; Parce, J. W.; Thomas, M. J.; Lyles, D. S. *Biochemistry* **1990**, *29*, 5734−5743.
(14) Packard, B.; Ediddin, M.; Komoriya, A. *Biochemistry* **1986**, *25*, 3548−3552.
(15) Timbs, M. M.; Thompson, N. L. *Biophys. J.* **1990**, *58*, 413−428.
(16) Forkey, J. N.; Quinlan, M. E.; Shaw, M. A.; Corrie, J. E. T.; Goldman, Y. E. *Nature* **2003**, *422*, 399−404.
(17) Friess, S. D.; Zenobi, R. *J. Am. Soc. Mass Spectrom.* **2001**, *12*, 810−818.
(18) Friess, S. D.; Daniel, J. M.; Zenobi, R. *Phys. Chem. Chem. Phys.* **2004**, *6*, 2664−2675.
(19) Gutman, M.; Huppert, D.; Nachliel, E. *Eur. J. Biochem.* **1982**, *121*, 637−642.
(20) Yam, R.; Nachliel, E.; Kiryati, S.; Gutman, M.; Huppert, D. *Biophys. J.* **1991**, *59*, 4−11.
(21) Cha, J. N.; Birkedal, H.; Euliss, L. E.; Bartl, M. H.; Wong, M. S.; Deming, T. J.; Stucky, G. D. *J. Am. Chem. Soc.* **2003**, *125*, 8285−8289.
(22) Bhatia, R. B.; Brinker, C. J.; Gupta, A. K.; Singh, A. K. *Chem. Mater.* **2000**, *12*, 2434−2441.

monitored at 505 nm, while fluorescein-labeled polymers were excited at 495 nm with emission monitored at 520 nm. All other parameters were adjusted as previously described.[9]

Time-resolved fluorescence intensity and anisotropy decay data were acquired in the time-domain using an IBH 5000U time-correlated single photon counting fluorimeter (Glasgow, UK), as described in detail elsewhere.[9] Pyranine-labeled samples were excited using a 455 nm NanoLED source (pulse duration at fwhm of 1.4 ns) with emission collected at 505 nm, while fluorescein-labeled samples were excited using a 495 nm NanoLED source with emission collected at 520 nm. The excitation band-pass was set to 16 nm, and the emission band-pass, to 32 nm. Appropriate short-pass and long-pass filters were employed in the excitation and emission path to avoid scattering effects.

The experimentally obtained parallel ($I_{VV}(t)$) and perpendicular ($I_{VH}(t)$) fluorescence decays were used to generate the sum, $S(t)$, difference, $D(t)$, and time-resolved anisotropy, $r(t)$, functions as follows:[23−25]

$$r(t) = \frac{I_{VV}(t) - GI_{VH}(t)}{I_{VV}(t) + 2GI_{VH}(t)} = \frac{D(t)}{S(t)} \quad (1)$$

where G is the polarization bias of the fluorescence detection system. The anisotropy decay was fit to a two-component hindered rotor model according to the following equation:[26]

$$r(t) = fr_0 \exp(-t/\phi_1) + (1 - f - g)r_0 \exp(-t/\phi_2) + gr_0 \quad (2)$$

where ϕ_1 reflects rapid rotational motions on the picosecond time scale, ϕ_2 reflects reorientation of probes on the nanosecond time scale, f is the fraction of fluorescence originating from ϕ_1, $(1 - f - g)$ is the fraction of fluorescence owing to ϕ_2, g is the fraction of fluorescence due to probes rotating slower than can be measured with fluorescein or pyranine ($\phi > 50$ ns), and r_0 is the time-zero or limiting anisotropy. In some cases, the value of gr_0 is denoted as r_∞, the residual anisotropy. Fits were considered acceptable if the reduced chi-squared (χ_R^2) was close to 1.0 and the weighted residuals were randomly distributed about zero.

Molecular Modeling: The structures of pyranine and the polyamines were constructed using a semiempirical Austin method (AM1) and Gaussian 98 software in Hyperchem.[27] Energies of the polymer chains and the N−N distances were minimized using Molecular Mechanics (MM+),[28] which is fairly crude but often used to model polymeric chains.[29] Energy minimizations were terminated when the energy difference between two successive iterations was less than 0.01 kcal mol^{-1}.

Results and Discussion

Polyamine−Probe Ionic Complexes. The formation of ionic complexes between fluorescent probes and polyelectrolytes has recently been described in detail[9,30] and is the basis for noncovalent labeling of proteins.[1,2,31] In this study, we used the anionic fluorescent probes fluorescein and pyranine in complex with homogeneous cationic polyamines to explore the effect of the mode of label attachment on the dynamic information obtained by TRFA. Ionic complexes of poly-D-lysine (PL), poly-L-ornithine (PO), poly-L-arginine (PR), poly-allylamine (PAM), and poly(ethyleneimine) (PEI) (0.05 wt %, 5 mM Tris-HCl, pH 8.3) with fluorescein and pyranine were formed at a polymer/probe mole ratio greater than 10:1 to ensure that no more than one probe was attached to a single polymer chain. PO, PL, and PR consist of a peptide backbone with alkyl side chains that increase in linear length by one rotatable bond (i.e., 4, 5, and 6 bonds, respectively). In addition, PO and PL both contain a single amino group through which ionic binding can occur, while ionic binding to the PR side chain can occur through interaction with the cationic guanidinium moiety. PAM and PEI polymers both have ethylene-based backbones that are significantly more rigid than the peptide-based polymers due to charge repulsion of the closely spaced amine groups.[32] The PAM side chain contains two rotatable bonds and a single primary amine through which ionic labeling can occur while PEI has no side chain and its secondary amino group mediates ionic labeling directly to the backbone. All the polyamines used were homogeneous to ensure uniform motions were present in the polymer−probe systems and were sufficiently long (>13 kDa) to minimize binding of the probe to the chain ends, where main-chain mobility is often greater than that in the center of the polymer chain.[33]

The ionic nature of the complexes was demonstrated by red shifts in the absorption spectra of these complexes relative to the spectra of free fluorescein (e.g., λ_{max}, 492 → 498 nm for PAM) or pyranine (e.g., λ_{max}, 455 → 459 nm for PAM; see supplementary Table S1).[9,30] The red shift observed for PAM−fluorescein was completely reversed by adding ~0.1 M KCl, while the red shift for PAM−pyranine was only partially reversed (λ_{max}, 459 → 457 nm), even at higher ionic strength (~1 M KCl; see supplementary Table S1), indicating stronger ionic binding of pyranine to PAM. Additionally, the two complexes showed a large difference in steady-state anisotropy values relative to each other (e.g., 0.091 ± 0.003 for PAM−fluorescein and 0.146 ± 0.004 for PAM−pyranine; see supplementary Table S2), which correspond to average rotational correlation times of 1.35 and 4.63 ns, respectively, for PAM−Fl and PAM−Pyr using $r_0 = 0.36$ and $\langle\tau\rangle = 4.0$ for PAM−Fl and $r_0 = 0.32$ and $\langle\tau\rangle = 5.7$ for PAM−Pyr (see supplementary Table S3). This indicates a more restricted mobility of the pyranine fluorophore when bound to PAM. Titration with KCl led to a reduction in steady-state anisotropy for both systems, but again a much higher concentration of KCl was required to significantly reduce the steady-state anisotropy value of pyranine-labeled polymers relative to fluorescein-labeled polymers (see supplementary Figure S1). Also noteworthy is the scaling of the steady-state anisotropy of pyranine with the shortening of the side chain length in the host polyamine (PL ≈ PO < PR < PAM < PEI), an observation which is explained in more detail below. Collectively, these differences between fluorescein-labeled and pyranine-labeled polyamines strongly suggest that pyranine forms a stronger electrostatic interaction with the polyamines than does fluorescein and that pyranine is more rigid when attached to the polyamine molecules.

Molecular Modeling of Probe−Polyamine Complexes. The potential for pyranine to undergo multipoint binding to the

(23) Demas, J. N. *Excited-State Lifetime Measurements*; Academic Press: New York, 1983.
(24) Lakowicz, J. R.; Gryczynski, I. *Topics in Fluorescence Spectroscopy*, Vol. 1; Plenum: New York, 1991.
(25) (a) Bright, F. V.; Betts, T. A.; Litwiler, K. S. *CRC Crit. Rev. Anal. Chem.* **1990**, *21*, 389−405. (b) Bright, F. V. *Appl. Spectrosc.* **1995**, *49*, 14A−20A.
(26) Geddes, C. D.; Karolin, J.; Birch, D. S. *J. Phys. Chem. B* **2002**, *106*, 3835−3841.
(27) Frisch, M. J. et al. *Gaussian 98*, revision A.9; Gaussian, Inc.: Pittsburgh, PA, 1998.
(28) Allinger, N. L. *J. Am. Chem. Soc.* **1977**, *99*, 8127−8134.
(29) Weiner, S. J.; Kollman, P. A.; Nguyen, D. T.; Case, D. A. *J. Comput. Chem.* **1986**, *7*, 230−252.
(30) Caruso, F.; Donath, E.; Mohwald, H.; Georgieva, R. *Macromolecules* **1998**, *31*, 7365−7377.
(31) Welder, F.; Paul, B.; Nakazumi, H.; Yagi, S.; Colyer, C. L. *J. Chromatogr., B* **2003**, *793*, 93−105.
(32) Itaya, T.; Ochiai, H. *J. Polym. Sci., Polym. Phys. Ed.* **1992,** *30*, 587−590.
(33) Debnath, P.; Cherayil, B. J. *J. Chem. Phys.* **2004**, *120*, 2482−2489.

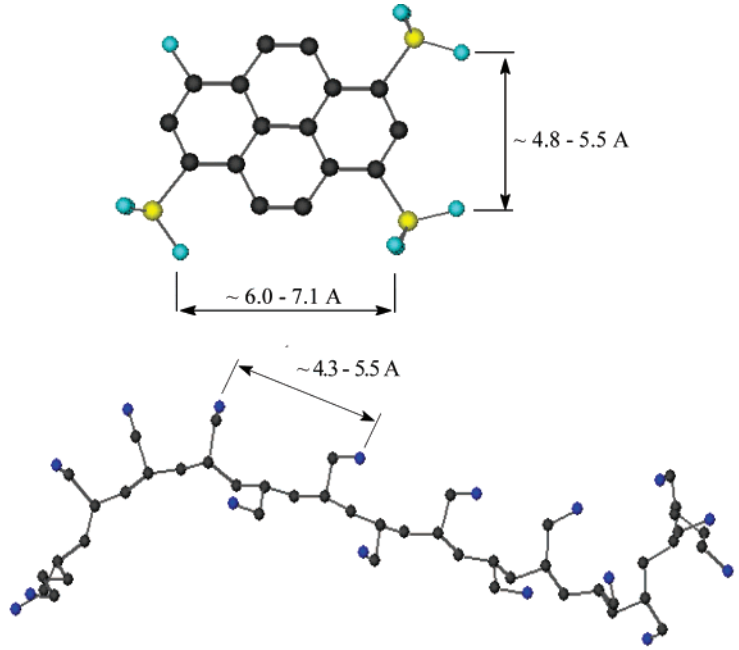

Homopolymer	N-N distance, Å	Sidechain Length
Poly-L-arginine	4.0 – 8.6	6
Poly-D-lysine	3.8 - 8.2	5
Poly-L-ornithine	4.6 – 7.8	4
PAM	4.3 – 5.5	2
PEI	4.5 – 5.0	0

Figure 1. Distances between adjacent sulfonate groups on pyranine and the N−N distance of two spatially close nitrogen atoms of the side chains calculated from the three-dimensional structures of a 16-member segment of PAM. N−N distances for other polyamines used are listed in the Table. Structures were optimized using the semiempirical AM1 method. Aromaticity in the benzene rings of pyranine was omitted for clarity.

polyamines was investigated by performing molecular mechanics calculations on pyranine and the different polyamines used in this study. Optimization of the three-dimensional structure of pyranine showed that the three highly acidic sulfonate groups ($pK_a \approx 0.5$[19]) are spaced ~4.8−5.5 Å apart along the short axis (i.e., sulfonate groups at positions 1 and 3) and ~6.0−7.1 Å apart along the long axis (i.e., sulfonate groups at positions 3 and 6) of the molecule (Figure 1). The distance between amino groups situated two positions apart (i.e., side chains i and $i + 2$) in a 16-member segment of the polyamines is within the same distance range according to molecular mechanics optimizations (Figure 1), in agreement with previous modeling of homogeneous polyamines using the Gaussian chain model.[34] The correlation in distances between the negatively charged sulfonates in the pyranine molecule and positively charged side chain groups in the polyamines suggests that pyranine is able to form a two-point ionic interaction with residues i and $(i + 2)$ along the polymer backbone. Since the N−N distances for the peptide based polymers match the distances between the sulfonate groups along both the long and short axis of the pyranine molecule, it is possible for the pyranine/polyamine complex to form with either the sulfonate groups at positions 1 and 3 or positions 3 and 6 paired with the positive charges on the polymer.

Because pyranine has three sulfonate groups there does exist the possibility for three-site binding of the pyranine to the charged polyamines. However, the sulfonate group that is free when pyranine forms a double-point ionic bond is located on the opposite side of the pyranine molecule (Figure 1), and its orientation relative to the closest ammonium group in the polymer would require considerable bending of the polymer backbone. Given the steric and geometrical requirements for this to occur and considering the limited overall flexibility of the backbone,[32,35,36] three-site binding of pyranine is unlikely, an assumption that is also supported by mass spectrometry of noncovalent complexes of proteins with trisulfonated pyrene receptors.[17] Hence, double-point binding of the pyranine probe to the cationic polymers is expected to be the dominant interaction.

In contrast to pyranine, fluorescein contains a moderately acidic carboxylate group and a much less acidic phenol group ($pK_a \approx 4.34$ and 6.68, respectively[37]). Therefore, the carboxylic acid is likely to be the only possible point of attachment to the amino side chain. Since a single ionic bond allows a considerable degree of rotation of the label around that bond, the probe motion would not be significantly compromised after binding. This explains the experimental data obtained for fluorescein-labeled polyamines. From these theoretical considerations and given the disparity in experimental data with respect to the reversibility of absorption shifts and the increased steady-state

(34) Kundrotas, P. J.; Karshikoff, A. *Biochim. Biophys. Acta* **2004**, *1702*, 1−8.
(35) Kobayashi, S.; Suh, K. D.; Shirokura, Y. *Macromolecules* **1989**, *22*, 2363−2366.
(36) Wittebort, R. J.; Szabo, A.; Gurd, F. R. N. *J. Am. Chem. Soc.* **1980**, *102*, 5723−28.
(37) Smith, S. A.; Pretorius, W. A. *Water SA* **2002**, *28*, 395−402.

anisotropy values for pyranine relative to fluorescein, the increased rigidity of the pyranine−polyamine complexes is attributed to pyranine being rigidly bound to the polyamines through two points of attachment.

Time-Resolved Fluorescence Anisotropy. TRFA data were collected to compare the information on rotational dynamics of polyamines labeled with different fluorophores: fluorescein vs pyranine. Also, the effect of subtle structural variations in the side chain length of polyamines on the TRFA decay parameters was studied. The intensity decay functions ($S(t)$ in eq 1) were essentially monoexponential; however, each probe did show a slight contribution from a second−and, in the case of PEI, a third−shorter lifetime component (∼2 ns for fluorescein and ∼3 ns for pyranine) that is likely due to a slight alteration of the charge on the probe as a result of ionic binding (Table S3; see Supporting Information).[9] The anisotropy decays were successfully deconvoluted into two time components, ϕ_1 and ϕ_2, for both fluorescein and pyranine complexes and showed a negligible residual anisotropy (r_∞), consistent with a high degree of polymer flexibility[38] and the absence of contributions from the overall polymer rotation in the measured decays (Figure 2). Comparison of the anisotropy decays for fluorescein- and pyranine-labeled PL, PR, and PAM shows that the fluorescence anisotropy decays more slowly for the polymer labeled with pyranine compared to fluorescein-labeled polymers, indicating a more rigid complex between pyranine and the polymers (Figure 2). The rigidity of the pyranine complex is dependent upon the polymer and hence the side chain group to which the probe is bound, as indicated by the different decay profiles for pyranine-labeled PL, PAM, and PR (Figure 2b, 2d, 2e, respectively) and the differences in the two time components derived from the slopes of the double exponential decay curves (Table S3).

(i) Side-Chain and Backbone Dynamics of Fluorescein-Labeled Polypeptides. The two rotational correlation times, ϕ_1 and ϕ_2 ($\phi_1 < \phi_2$) obtained from the fit of TRFA decay to a biexponential function (eq 2) have been attributed to the motion of the side chain segment to which the probe is bound and the motion of a short segment of the polymer backbone, respectively.[9] Because the probe-binding site involves the side chain of the polymer, the freedom of the probe to undergo independent motion relative to the polymer is reflected in the shorter correlation time, ϕ_1. Hence, ϕ_1 can be used as an indicator of the rigidity of the interaction between the probe and the polymer; that is, a larger ϕ_1 value signifies a more rigid interaction.

Both fluorescein-labeled PO and PL showed very short correlation times (∼0.20 ns) that likely result from the long side chain and the high flexibility due to the large number of degrees of freedom (Figure 3). The ϕ_1 values are significantly increased when side chain length and flexibility are reduced, as seen, for example, from the ϕ_1 correlation time for PAM (∼0.56 ns), where the side chain contains only 2 degrees of freedom and flexibility of the side chain is hindered. Notably, PR also shows a significant reduction in ϕ_1 (∼2-fold) relative to the other peptide-based polymers despite having a longer side chain (6 atoms linearly) and more degrees of freedom. This result likely reflects the rigidity of the planar geometry of the guanidinium group at the end of the arginine side chain, causing the probe to become more rigid and less mobile. Interestingly, the ϕ_1 correlation time for the fluorescein−PEI system, which lacks a side chain, shows the presence of very fast depolarization ($\phi_1 = 170$ ps) which is consistent with a small fraction (∼12%) of unbound probe that is rotating freely in solution (see supplementary Table S3).

To determine how well the ϕ_2 component reflects the segmental dynamics of the labeled macromolecules, we have compared the measured ϕ_2 values for the peptide-based polymers to previous ^{13}C NMR relaxation measurements.[39−42] Several previous studies have shown that while both NMR and TRFA methods can yield identical rotational correlation times,[43,44] in many cases, rotational correlation times determined by TRFA are shorter than those obtained from NMR data,[45,46] likely due to the effect of independent probe motions in fluorescence experiments. The averaged rotational correlation time for C_α atoms in PL measured by ^{13}C NMR at 28 °C in water is ∼4.5 ns.[36] In the present study the ϕ_2 values obtained by TRFA were in a range of ∼1.5 ns for all the fluorescein-labeled polymers with the exception of PAM, which showed a ϕ_2 value of ∼3.7 ns (Figure 3). The higher ϕ_2 value for PAM is expected, however, given the rigidity of the backbone imparted by the closely spaced amine groups on the side chain.[32] These results indicated that the ϕ_2 obtained for the fluorescein-labeled peptides by TRFA is ∼3-fold shorter than the correlation times obtained in NMR experiments, a result that highlights the significant decoupling of the probe motion from the polymer segmental motion, as expected given the short picosecond motion of the long side chains. Importantly, shortening of the side chain for these polymers had no significant effect on the ϕ_2 values of the peptides, as the three peptides showed similar correlation times despite the differences in side chain length (Figure 3). Hence, for probes bound through a single ionic bond it is not possible to accurately determine the rates of protein segmental motions, in agreement with previous studies involving covalently bound probes.[45,46]

(ii) Side-Chain and Backbone Dynamics of Pyranine-Labeled Polymers. With the exception of PEI, ionic labeling of the polymers with pyranine resulted in a ∼2−3-fold increase in the side chain correlation time, ϕ_1, relative to those seen with fluorescein-labeled polymers, regardless of side chain length (Figure 3). The observed slower motion of the side chain in general is in agreement with steady-state anisotropy data and is indicative of more rigid binding of the probe to the polymer owing to the double-point binding between pyranine and the polymers.[7,18,20] Specifically, PAM and PEI both show a ϕ_1 value in the nanosecond range ($\phi_1 = 1.25$ ns and 1.29 ns, respectively) while the peptide-based polymers show significantly longer ϕ_1 values (∼0.60−0.90 ns) compared to fluorescein-labeled peptides (∼0.20−0.45 ns; Figure 3). In all cases the fractional contribution, f_1, slightly decreases for pyranine-labeled polymers relative to fluorescein-labeled polymers, giving a further

(38) Spyros, A.; Dais, P.; Heatley, F. *Macromolecules* **1994**, *27*, 5845−5857.
(39) Ishima, R.; Torchia, D. A. *Nat. Struct. Biol.* **2000**, *7*, 740−743.
(40) Palmer, A. G. *Annu. Rev. Biophys. Biomol. Struct.* **2001**, *30*, 129−55.
(41) Columbus, L.; Hubbell, W. L. *Trends Biochem. Sci.* **2002**, *27*, 288−295.
(42) Eisenmesser, E. Z.; Millet, O.; Labeikovsky, W.; Korzhnev, D. M.; Wolf-Watz, M.; Bosco, D. A.; Skalicky, J. J.; Kay, L. E.; Kern, D. *Nature* **2005**, *438*, 117−121.
(43) Moncrieffe, M. C.; Juranic, N.; Kemple, M. D.; Potter, J. D.; Macura, S.; Prendergast, F. G. *J. Mol. Biol.* **2000**, *297*, 147−163.
(44) Alexiev, U.; Rimke, I.; Pöhlmann, T. *J. Mol. Biol.* **2003**, *328*, 705−719.
(45) Palmer, A. G.; Hochstrasser, R. A.; Millar, D. P.; Rance, M.; Wright, P. E. *J. Am. Chem. Soc.* **1992**, *115*, 6333−6345.
(46) Kemple, M. D.; Buckley, P.; Yuan, P.; Prendergast, F. G. *Biochemistry* **1997**, *36*, 1678−88.

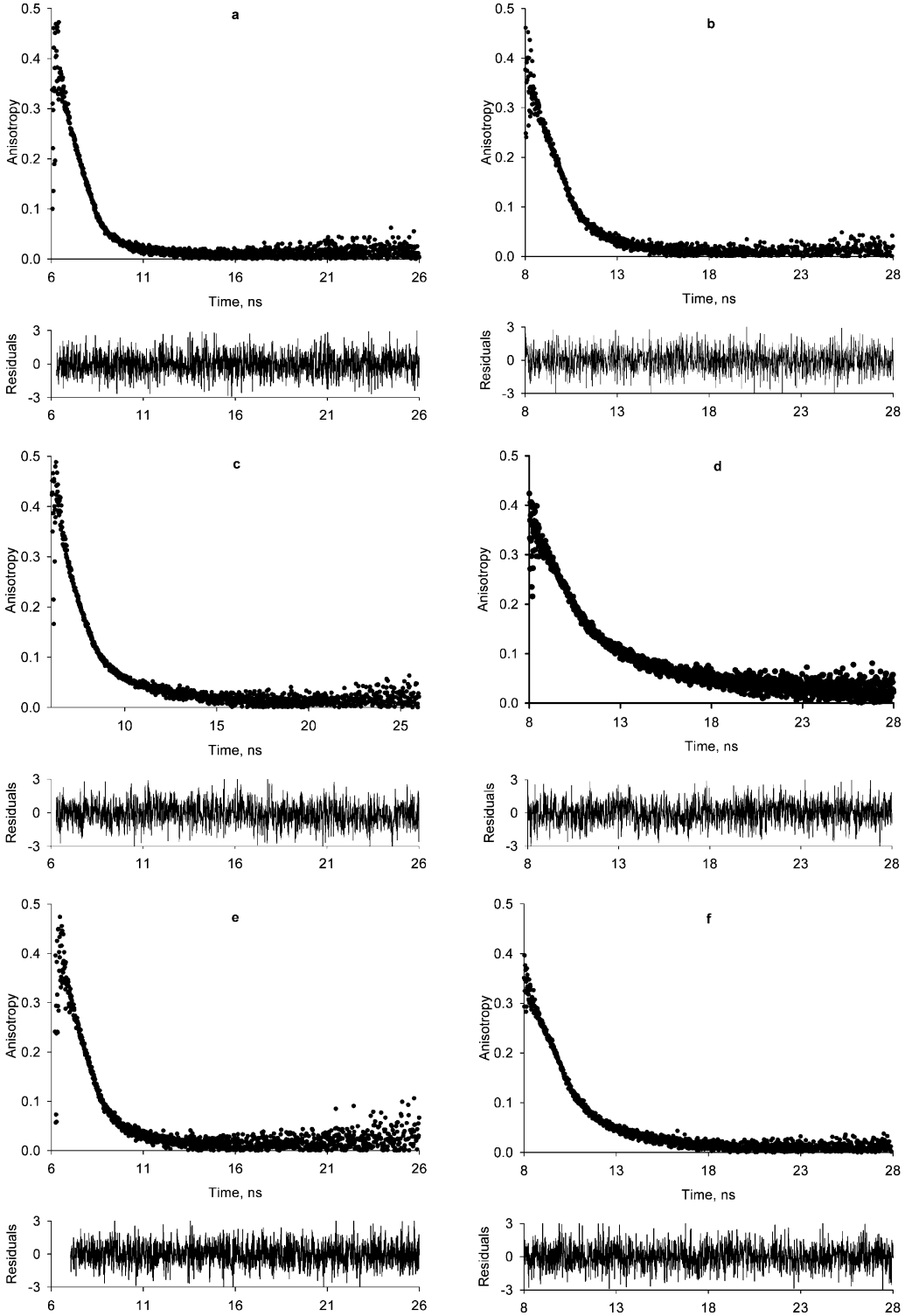

Figure 2. Time-resolved anisotropy decays and residual plots for difference fits of (a) PL−fluorescein; (b) PL−pyranine; (c) PAM−fluorescein; (d) PAM−pyranine; (e) PR−fluorescein; and (f) PR−pyranine. Solvent, 5 mM Tris-HCl, pH 8.3; 0.05% peptide concentration; 1.4 μM fluorescein; 2 μM pyranine. Plots (a) and (c) have been published previously[9] and are shown for comparison.

indication that the local probe motions are reduced for all polymers when labeled with pyranine.

As was the case with the side chain correlation times, Figure 3 shows that, with the exception of PEI, labeling of the peptide-based polymers with pyranine led to roughly a ∼2−3-fold increase in the ϕ_2 correlation times relative to those obtained with fluorescein-labeled polymers. The overall increase in both the value and fractional contribution of ϕ_2 results from the ability of pyranine to form a more rigid complex with the polymers (as indicated by the increased ϕ_1 correlation times), which in turn leads to improved coupling of the probe to the backbone motion of the polymers. More importantly, the ϕ_2 values determined from TRFA analysis of pyranine-labeled peptides more accurately reflect the backbone correlation times measured by NMR spectroscopy ($\phi = 4.5$ ns), particularly in the case of PR ($\phi_2 = 4.0$ ns). Poorer agreement was observed for PO

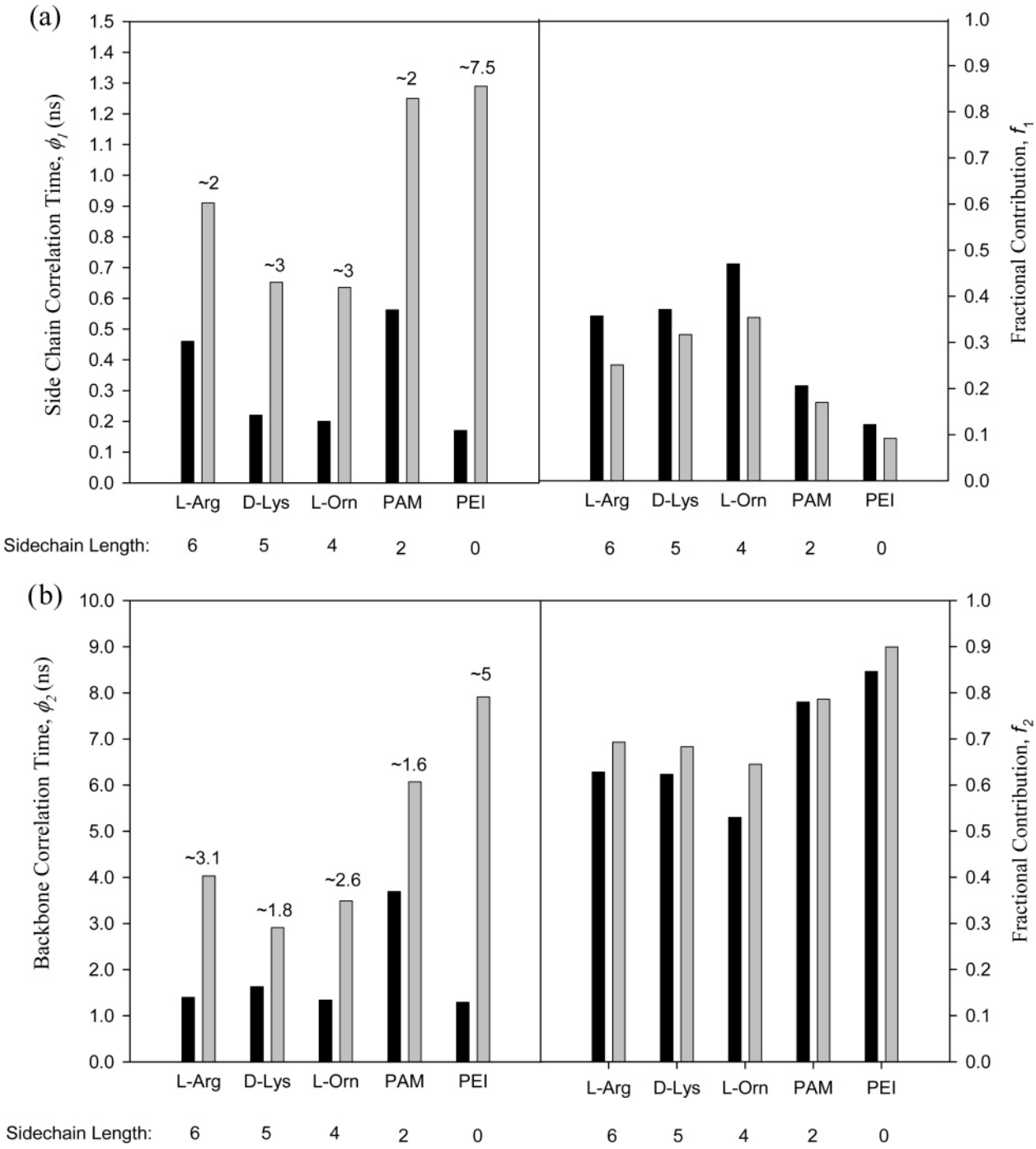

Figure 3. Comparison of time-resolved fluorescence anisotropy data for (a) side-chain and (b) backbone motions using single-point (black) and double-point (gray) ionic labeling with fluorescein and pyranine, respectively. Left panels show correlation times; right panels show fractional contributions. Data for fluorescein-labeled PL and PAM were previously published[9] and are shown for comparison.

($\phi_2 = 3.5$ ns) and PL ($\phi_2 = 2.9$ ns), consistent with the greater degree of motion for these side chains relative to the side chains in PR. Taken together, these results suggest that the ability of pyranine to couple to the backbone motion of the polymer is improved as the length of the side chain to which the probe is attached decreases. It is worth noting that double-point labeling does not lead to artificial restriction of the backbone motion, as indicated by the very low g-value obtained in solution ($g < 0.05$ in all cases) and the fact that the backbone correlation times are lower than those seen in NMR experiments.

It is important to further consider the TRFA results obtained for pyranine-labeled PR. On the basis of chain length alone, one should expect a lower ϕ_1 value and hence less rigid coupling of the probe to the backbone motion relative to PL or PO, which is opposite to the data obtained. The origin of the increased ϕ_1 value for pyranine-labeled PR could be due to the planarity of the guanidinium group at the end of the arginine side chain or the ability of arginine to form a bidentate "ring-structured" salt bridge with a single sulfonate group.[47,48] The latter scenario is thought to be responsible for the increased specificity between arginine side chains and sulfonate dyes[17,18] and, in the current study, provides the opportunity for four potential points of

(47) Ichimura, S.; Mita, K.; Zama, M. *Biopolymers* **1978**, *17*, 2769−2778.
(48) Condie, C. C.; Quay, S. C. *J. Biol. Chem.* **1983**, *258*, 8231−8234.

contact between the pyranine molecule and the side chains in PR (two per side chain), facilitating a much stronger and more rigid interaction between the probe and polymer. This highlights the fact that both chain length and chain rigidity influence the coupling of the probe to the backbone and suggests that optimal coupling of pyranine to proteins should be obtained for proteins containing appropriately spaced Arg residues on their surface.

TRFA data for pyranine complexes with PAM and PEI also warrant further discussion. In the case of PAM, the side chain length is minimal and the proximity of the charged side chains provides a rigid connection between the probe binding site and the polymer backbone. This provides optimal conditions for pyranine coupling to the backbone motion of the polymer, which is supported by the high fractional contribution of the ϕ_2 correlation time of the polymer (~78%) when labeled with pyranine. Interestingly, the fractional contribution for ϕ_2 observed for fluorescein-labeled PAM was approximately the same, indicating that both fluorescein and pyranine are well coupled to the backbone motion of PAM, likely due to the rigidity and short side chain length. A difference in the ϕ_2 correlation times for fluorescein- (ϕ_2 ~3.69 ns) and pyranine- (ϕ_2 ~6.07 ns) labeled PAM highlights the effect that rapid local motions in the fluorescein-labeled polymer systems have on observing the true segmental motion of the polymers.

As shown in Figure 3, the difference in ϕ_1 and ϕ_2 was particularly large for fluorescein- and pyranine-labeled PEI, which has no side chain. Despite the lack of a side chain, a significant fraction of a relatively fast motion (9% of a 1.3 ns component) remained when PEI was labeled with pyranine (Figure 3). The slower correlation time relative to fluorescein (170 ps) suggests that this is not due to a fraction of pyranine that is bound through a single site. Furthermore, the significant increase in ϕ_2 for pyranine ($\phi_2 = 7.9$ ns) relative to fluorescein ($\phi_2 = 1.3$ ns) supports the binding of pyranine through two sites. The small fraction of relatively rapid motion for pyranine-bound PEI is thus most likely due to "wobbling" of the dye around the long axis of the polymer, which will not be completely restricted when only two bonds form between the dye and polymer chain. Clearly, increases in chain length will result in significant increases in the degree of wobbling motion, combined with torsional motion owing to the potential for rotation of bonds in the longer side chains. This leads to the observed increase in fractional contribution and decrease in ϕ_1 for the other pyranine−polymer systems as chain length increases.

Behavior of Fluorescein− and Pyranine−Polymer Systems Entrapped in Silica: To demonstrate the utility of TRFA measurements using pyranine-labeled polymers, we reinvestigated the dynamics of two model polyamines when entrapped in sol−gel derived silica. A previous study of fluorescein-labeled PL and PAM entrapped in sodium silicate derived hydrogels showed that the entrapment of PAM−fluorescein in sodium silicate resulted in a significant increase in ϕ_2 relative to solution (e.g., 3.7 ns in solution vs 10.7 ns in sodium silicate), while the mobility of entrapped PL appeared to be almost identical to that in solution.[9] The latter result was not expected, given that PL should show significant dampening of motion owing to electrostatic interactions with the silica surface. Indeed, such interactions have been utilized in the templating of silica to form mesostructured materials.[49]

The above results were initially attributed to the increased flexibility of PL relative to PAM as a result of increased spatial freedom for flexion of the peptide backbone within the pores formed in PL doped silica. Evaluation of the pore size distributions in PL templated silica materials by Hawkins et al., however, revealed average pore sizes in a range of 1.5 nm for silica materials synthesized using α-helical PL as a templating agent.[49] Furthermore, materials derived from PL in the random coil conformation revealed a much lower surface area and total pore volume, suggesting that the mobility of PL would be considerably restricted in these materials due to the confinement imparted by the small pores. These findings, together with the fact that PL should be electrostatically adsorbed to the anionic pore walls in silica hydrogels, strongly suggests that the PL polymer ought to demonstrate considerable restricted motion relative to that seen in solution and has prompted us to revisit the behavior of polyamines entrapped in sodium silicate.

In contrast to the fluorescein-labeled PAM and PL, PAM and PL labeled with pyranine both showed a significant restriction in motion upon entrapment in sodium silicate, as seen by the high residual anisotropy of the entrapped polyamines relative to solution (Figure 4, top). This is in contrast to the results seen previously with encapsulated fluorescein-labeled polymers, which showed a high fraction of hindered motion for PAM but not for PL (Figure 4, bottom). The significant amount of hindered motion observed for entrapped Pyr−polymer complexes is consistent with the expected binding of the polymers to the silica surfaces, and thus the apparent mobility of fluorescein-labeled PL (and PAM) is consistent with the inability of fluorescein to effectively couple to the segmental motion of the polymer.

In accordance with the increased *g*-value, the ϕ_2 value for pyranine-labeled PL showed evidence of decreased mobility upon entrapment ($\phi_2 = 10.3$ ns in silica vs 2.9 ns in solution; Figure 5, right). The ~10 ns backbone correlation time for entrapped pyranine-labeled PL is, again, markedly different from that obtained for the entrapped fluorescein-labeled species, which previously showed a ϕ_2 value of 4.0 ns.[9] Interestingly, pyranine-labeled PAM also showed an increase in the backbone correlation time (ϕ_2 ~41ns) compared to the entrapped fluorescein labeled species (ϕ_2 ~10.6 ns) further highlighting the effect that local probe motions have on the correct interpretation of anisotropy decay data (Figure 5).

Collectively, the increase in *g*-value and backbone correlation times indicates that there is indeed a significant reduction in polymer mobility for both PL and PAM resulting from the electrostatic interaction between the polymer and the silica surface. It is worth noting that entrapped PAM shows a higher degree of hindered motion (g ~0.8) relative to entrapped PL ($g = 0.6$) and a higher ϕ_2 value (41 ns vs 10.3 ns), indicating that the reduction in mobility upon entrapment is dependent on the degree of polymer flexibility, in keeping with our initial findings.[9] This is likely due to more efficient templating of the silica around the more rigid PAM polymer, a process that would be inherently less efficient for more flexible species such as PL. It is worth mentioning that the current results support our original hypothesis that more flexible polyamines retain a higher degree of flexibility compared to more rigid polymers when

(49) Hawkins, K. M.; Wang, S. S.; Ford, D. M.; Shantz, D. F. *J. Am. Chem. Soc.* **2004**, *126*, 9112−9119.

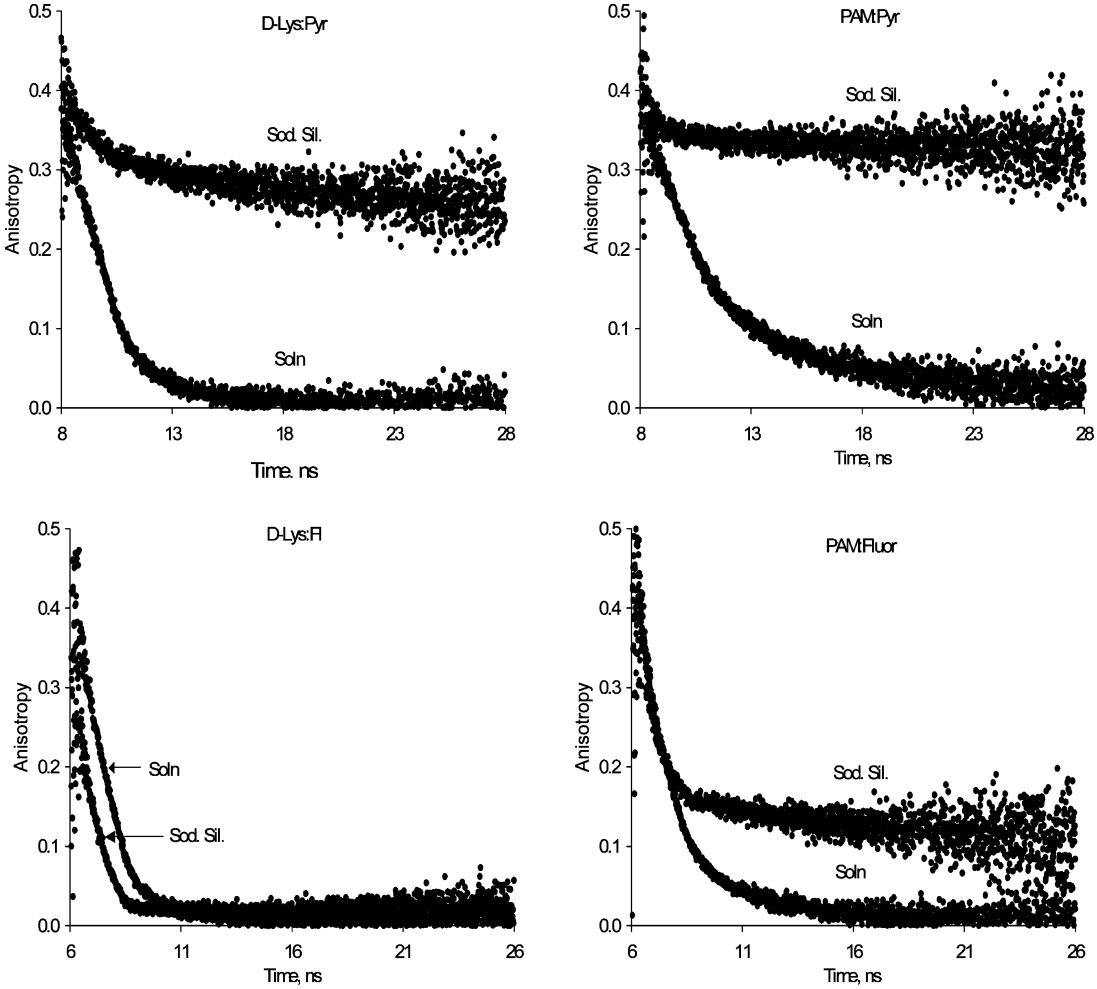

Figure 4. Comparison of anisotropy decays for fluorescein- and pyranine-labeled PL and PAM entrapped in sodium silicate hydrogels. The pyranine-labeled species (top) show a large degree of restricted motion compared to previous studies with the fluorescein-labeled polymers (bottom) (from ref 9).

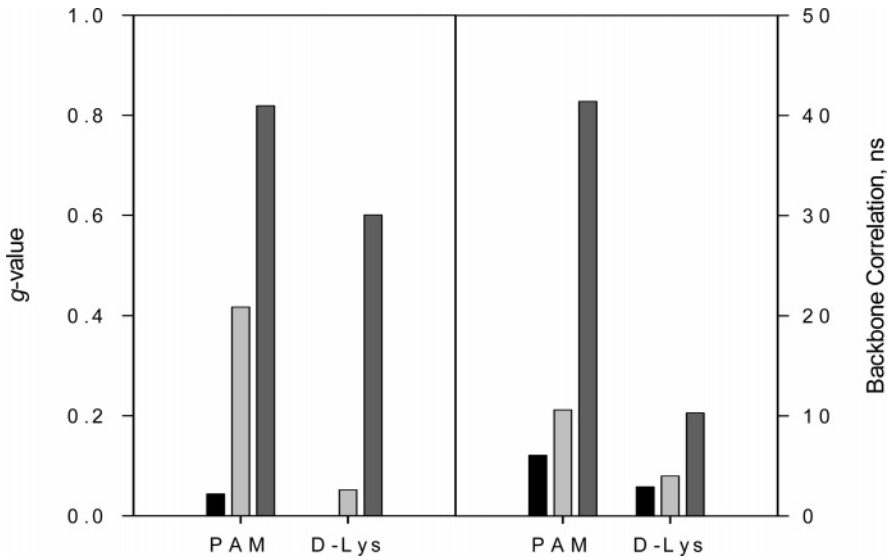

Figure 5. Comparison of g-values (left) and backbone correlation times, ϕ_2, (right) for Pyr−PL and Pyr−PAM complexes in solution (black), fluorescein−PL and fluorescein−PAM in sodium silicate (light gray, from ref 9), and Pry−PL and Pyr−PAM in sodium silicate (dark gray).

entrapped;[9] however, the difference is clearly not nearly as great as we originally predicted.

The ability to accurately assess the segmental motion of polymers within silica is likely to have significant ramifications in future studies of pyranine-labeled proteins within such materials. Currently, there is a large body of literature on protein dynamics in silica, a great deal of which has relied on the use of fluorescence spectroscopy[50−52] owing to the small amount of protein contained in these materials, which precludes NMR dynamics studies.[53] These studies often provide contrasting

views on the effects of encapsulation on protein mobility within silica, perhaps due in part to the fact that such studies usually employ probes that are bound through a single bond. It is possible that proteins are in fact much less mobile in silica than is currently thought, a possibility that could have implications in the overall function of these systems, given the importance of dynamic motions in protein function.[42,54] To our knowledge, no two-point labeling technique (covalent or noncovalent) has been applied to study protein dynamics in sol−gel materials. Clearly, the potential to noncovalently label proteins through a two-point interaction will provide a new tool for probing protein dynamics within silica and is likely to result in new insights into the nature of protein−silica interactions and the effects of protein dynamics on activity.

Implications of Two-Point Ionic Labeling. The side group mobility and its relation to the backbone chain dynamics measured by TRFA is a complex problem recently addressed by Duhamel.[55] The important conclusion from those studies is that a residue located inside the polymer coil probes only a finite volume of the polymer. As a first approximation, the polymer can be described as a consistent, flexible model of interconnected rigid bonds, and the probe, as a fast-rotating species fixed at one terminal bond. The rotation of the probe can be completely uncoupled from the polymer movement by using a long, flexible connection separating it from the rest of the polymer.[8−10,55] We have shown that even in cases where the probe is attached by a short linker (e.g., PAM and PEI), the possibility of rapid probe motions skewing the interpretation of fluorescence anisotropy data still exists when the probe is attached through a single bond.

Covalent bifunctional probes have been used previously to minimize the effects of independent probe motions in both EPR[13] and fluorescence experiments.[14,15] The synthesis of improved bifunctional fluorescent probes has also provided tools for determining specific structural features of a protein, including subunit orientation,[11] and effective methods to label specific recombinant proteins to more effectively monitor intracellular activity.[56] However, despite the clear advantages of these probes for accurately determining the rotational motions of biomolecules, fluorescent probes utilizing two points of attachment have not yet been widely used in TRFA experiments aimed at studying segmental protein motions, likely because the majority of these probes require surface-accessible cysteine residues that are appropriately spaced for labeling.

The present study represents the first successful use of a fluorescent probe attached via two ionic bonds to study backbone segmental motions using TRFA. Improved coupling to the polymer motion was demonstrated based on improved correlation with NMR dynamics data, even in the presence of a long linker. Furthermore, the method was amenable to studies of both free and entrapped polymers, highlighting the versatility of the labeling method. This technique provides a specific advantage over the covalent dimaleimide probes in that the positively charged sidegroups that are required for the two-point interaction to occur are prevalent on the surface of a protein. Indeed, even though the chain lengths of Lys and Arg groups are 5 and 6 carbons, respectively, double-point binding to these groups leads to significant improvements in coupling of the probe to the backbone motion. Given that several proteins, including lysozyme, cytochrome *c*, RNAse A, myoglobin, adenylate kinase, aldolase, and HSA, have been shown to have greater than 1:1 binding stoichiometry between amino groups and sulfonated dyes,[18−20] it is likely that this labeling method should be widely applicable. In comparing Lys to Arg, the latter shows significantly better coupling of the probe to the biomolecule, and our results indicate that the double-point ionic interaction between pyranine and PR is preserved up to 150 mM ionic strength, while that for PL is not, suggesting that selective labeling of Arg should be possible when operating under physiological conditions. Thus, proteins with R−X−R motifs are likely to be best suited to TRFA studies using ionically bound pyranine. While such a motif is not generically present in all proteins, incorporation of such a motif should be relatively straightforward using recombinant methods. Thus, the two-point labeling method should be applicable to a wide range of proteins.

Acknowledgment. The authors thank the Natural Sciences and Engineering Research Council of Canada, MDS-Sciex, the Ontario Ministry of Energy, Science and Technology, the Canada Foundation for Innovation, and the Ontario Innovation Trust for support of this work. J.D.B. holds the Canada Research Chair in Bioanalytical Chemistry.

Supporting Information Available: Tables showing absorbance, steady-state anisotropy, and TRFA data for polymer−probe complexes, a Figure showing the effect of ionic strength on the steady-state anisotropy of polymer−probe complexes, and complete ref 27. This material is available free of charge via the Internet at http://pubs.acs.org.

JA058707E

(50) Jordan, J. D.; Dunbar, R. A. Bright, F. V. *Anal. Chem.* **1995**, *67*, 2436−2443.
(51) Gottfried, D. S.; Kagan, A.; Hoffman, B. M.; Friedman, J. M. *J. Phys. Chem. B* **1999**, *103*, 2803−2807.
(52) Sui, X.; Cruz-Aguado, J. A.; Chen, D. Y.; Zhang, Z.; Brook, M. A.; Brennan, J. D. *Chem. Mater.* **2005**, *17*, 1174−1182.
(53) Brennan, J. D. *Appl. Spectrosc.* **1999**, *53*, 106A−121A.
(54) Basner, J. E.; Schwartz, S. D. *J. Am. Chem. Soc.* **2005**, *127*, 13822−13831.
(55) Duhamel, J.; Kanagalingam, S.; O'Brien, T. J.; Ingratta, M. W. *J. Am. Chem. Soc.* **2003**, *125*, 12810−12822.
(56) Girouard, S.; Houle, M. H.; Grandbois, A.; Keillor, J. W.; Michnick, S. W. *J. Am. Chem. Soc.* **2005**, *127*, 559−566.